ARTICLE

Extreme Condition High Temperature and High Pressure Studies of the K-U-Mo-O System

Received 00th January 20xx,
Accepted 00th January 20xx

DOI: 10.1039/x0xx00000x

Gabriel L. Murphy,*[a] Philip Kegler,[a] Martina Klinkenberg,[a] Shuao Wang[b] and Evgeny V. Alekseev*[a]

Herein the first examples of alkali earth uranyl molybdates synthesised using extreme conditions of high temperature and high pressure (HT/HP) methods, namely $K_2[UO_2(Mo_2O_7)_2]$, $K_2[(UO_2)_2(Mo(VI)_4Mo(IV)(OH)_2)O_{16}]$, $K_3[(UO_2)_6(OH)_2(MoO_4)_6(MoO_3OH)]$ and $K_5[(UO_2)_{10}MoO_5O_{11}OH]\cdot H_2O$, are described and characterised. $K_2[UO_2(Mo_2O_7)_2]$ forms a monoclinic 2D layered structure in space group $P2_1/c$ that consists of interlinking Mo_2O_7 dimers that link isolated UO_2^{2+} moieties forming $[UO_2(Mo_2O_7)_2]^{2-}$ layers which are separated by K^+ cations. $K_2[(UO_2)_2(Mo(VI)_4Mo(IV)(OH)_2)O_{16}]$ forms a disordered triclinic 3D framework structure in space group $P\bar{1}$. The structure consists of isolated UO_2^{2+} moieties connected in a layered configuration via $Mo(VI)O_6$ polyhedra of which the layers are bridged by $Mo(IV)O_6$ polyhedra that are partially positionally disordered by charge balancing K^+ and bridging Mo^{6+} cations. $K_3[(UO_2)_6(OH)_2(MoO_4)_6(MoO_3OH)]$ adopts a disordered orthorhombic 3D framework structure in space group *Pbcm* consisting of small channels and large cavities built upon corner sharing MoO_4 and UO_2^{2+} moieties that respectively encapsulate ordered and disordered K^+ cations. $K_5[(UO_2)_{10}MoO_5O_{11}OH]\cdot H_2O$ forms a triclinic 3D framework structure in space group $P\bar{1}$ consisting of interlinking UO_6, UO_7 and MoO_5 polyhedra which utilise cation-cation interactions between UO_2^{2+} moieties to create infinite channels parallel to the [001] direction which contain partially disordered K^+ cations and H_2O molecules. A combination of single crystal X-ray diffraction, bond valence sums calculations and scanning electron microscopy with energy dispersive X-ray spectroscopic measurements were used to characterise all obtained samples in this investigation. The structures uncovered in this investigation are discussed systematically in detail with other members of the broader A^+-U-Mo-O system from literature where the relationship between the degree of pressure applied and U/Mo ratio used during synthesis on the ability to obtain high dimensional structures via condensation and oligomerization of polyhedra is identified and discussed in detail.

Introduction

Molybdate based compounds have endured significant and sustained interest due to their broad applicability in societally important materials including catalysts,[2] optics,[3] oxide ion and proton conductors[4] in addition to their notable negative thermal expansion[5] properties. Core to these diverse applications is the ability for molybdenum to adopt a range of oxidation states, possess a variety of coordination environments and further potential to oligomerize with other Mo units which enables a rich array of structural types and topologies to be obtained. A topical feature of contemporary molybdate material investigation is the application of high pressure in both *in situ* structural and synthesis experimentations.[6-8] These investigations have highlighted the flexibility molybdate units have towards facilitating phase transformations and novel structure formation through the application of pressure. This has often resulted in the acquisition of unique materials not found under ambient pressure conditions and possessing novel properties and topologies pertinent in the context of general inorganic science.[5, 9]

Molybdenum forms as a fission daughter with a considerable yield during the operation of nuclear reactors.[10] Consequently, it has been of long-standing interest to examine potential structural phases that may occur between molybdenum, uranium and other actinides as this may impact reactor performance, spent nuclear fuel (SNF) repository operations and planning assessment.[11] Indeed such work has been progressed particularly through utilising high temperature and hydrothermal synthesis methods in the cases of Th, U, Np and Pu.[1, 12-14] In supporting the fundamental basis of SNF chemical behaviour, these studies have further highlighted the novel and rich properties actinide molybdates possess in addition to other systems.[12, 15-19] Although there are many studies at ambient to moderate pressure conditions particularly those pioneered by Burns and Albrecht-Schmidt and co-workers, there is a paucity of information for higher pressures, > 1 GPa, in which there are apparently no reports of high pressure derived uranyl molybdate phases.

A salient example of exploring the exotic chemistry of actinides with molybdates under high pressure conditions was demonstrated by Xiao *et al.*[20] in examining thorium molybdates. They demonstrated the remarkable structural flexibility present in $ThMo_2O_8$, of which when exposed to elevated pressures is able to undergo a phase

[a] 1Institute of Energy and Climate Research, Forschungszentrum Jülich GmbH, 52428 Jülich, Germany.
[b] 2State Key Laboratory of Radiation Medicine and Protection, School for Radiological and Interdisciplinary Sciences (RAD-X) and Collaborative Innovation Center of Radiation Medicine of Jiangsu Higher Education Institutions, Soochow University, Suzhou 215123, China

transformation resulting in an approximate 20 % volume reduction. This dramatic change was attributed to the versatile MoO_4 units which are able to readily conform to, and facilitate, the volume reduction. The chemistry of the more spherical Th(IV) cation compared to U(VI) is markedly different, where the occurrence of the hexavalent uranyl oxo group, UO_2^{2+}, brings added structural complexity that which can lead to more exotic chemical behaviour such as geometric isomerism[21] and charge transfer effects[22] and further result in interesting and significant bulk properties.

We have recently began a systematic investigation into the structure-property relationships of novel SNF related actinide phase formation under variable conditions.[21, 23] In the course of this investigation we have systematically examined the formation of a series potassium uranium molybdates when exposed to high temperature high pressure (HT/HP) conditions of 900 °C and 4 GPa. The structures uncovered show significant structural variation to that previously encountered in the A^+-U(VI)-Mo-O (A = alkali metal cation) system stemming from the flexibility of molybdate units. The novel structures; $K_2[UO_2(Mo_2O_7)_2]$, $K_2[(UO_2)_2(Mo(VI)_4Mo(IV)(OH)_2)O_{16}]$, $K_3[(UO_2)_6(OH)_2(MoO_4)_6(MoO_3OH)]$ and $K_5[(UO_2)_{10}MoO_5O_{11}OH]\cdot H_2O$ are characterised using single crystal X-ray diffraction and scanning electron microscopy/energy dispersive X-ray spectroscopy. The results are discussed with respect to the structural chemistry of the broader A^+-U(VI)-Mo-O system with particular regard to the ability for pressure to drive the formation of higher dimensional structures than those encountered at ambient, a result of greater coercion of polyhedra to undergo oligomerization and condensation.

Experimental

High Temperature/High Pressure Synthesis

High temperature/high pressure (HT/HP) syntheses was undertaken using a piston cylinder module of a combined piston cylinder / multi anvil apparatus (Voggenreiter LP 1000-540/50) located at IEK-6, Forschungszentrum Jülich, Germany. In all synthesis experiments a maximum temperature and pressure of respectively 900 °C and 4 GPa was used consistently. Experimental procedure of the HT/HP experiment is similar to that described in previous work.[23] For these experiments stoichiometric ratios of MoO_3 (Alfa Aesar, 99.9%), $UO_2(NO_3)_2{\cdot}6H_2O$ (International Bioanalytical Industries, Inc. 99%) and KNO_3 (Alfa Aesar, 99.9%) were mixed together thoroughly in an agate mortar and pestle prior to loading into platinum crucibles, and sealed. Table 1 describes the specific molar ratios used for the synthesis of compounds.

Single Crystal X-ray Diffraction

Suitable quality crystals were selected for analysis and structural refinement using single crystal X-ray diffraction (SC-XRD). Data were recorded with CrysAlisPro software on an Agilent Oxford Diffraction Super Nova diffractometer with a Mo Kα tube at 296 K. Absorption corrections for the raw data were performed using the multi-scan method. The unit cells were determined, and background effects were processed by the CrysAlisPro software. The initial structures were refined through using SHELXL-2018 within the WinGX (v1.80.05) software,[24] and the ADDSYM algorithm of the PLATON program[25] was used for the checking of possible higher symmetries. Data and crystallographic information for all compounds investigated are presented in Table 2. All structures reported in this work have been submitted to the Cambridge Crystallographic Data Centre (CCDC) under the numbers 2032068, 2032067, 2032070 and 2032071 for $K_2[UO_2(Mo_2O_7)_2]$, $K_2[(UO_2)_2(Mo(VI)_4Mo(IV)(OH)_2)O_{16}]$, $K_3[(UO_2)_6(OH)_2(MoO_4)_6(MoO_3OH)]$ and $K_5[(UO_2)_{10}MoO_5O_{11}OH]\cdot H_2O$ respectively. Due to disordering associated with anions and cations and also heavy atoms, residual electronic density was often encountered in the structural models.

Table 1. Molar ratios used for the synthesis of the title compounds using HT/HP conditions at 900 °C and 4 GPa.

Compound	MoO_3	$UO_2(NO_3)_2{\cdot}6H_2O$	KNO_3
$K_2[UO_2(Mo_2O_7)_2]$	4	1	10
$K_2[(UO_2)_2(Mo(VI)_4Mo(IV)(OH)_2)O_{16}]$	5	2	10
$K_3[(UO_2)_6(OH)_2(MoO_4)_6(MoO_3OH)]$	8	6	10
$K_5[(UO_2)_{10}MoO_5O_{11}OH]\cdot H_2O$	1	10	10

Scanning Electron Microscopy/Energy Dispersive X-ray Spectroscopy

The morphology and elemental composition of the crystals were determined using a FEI Quanta 200F Environment Scanning Electron Microscope (SEM) fitted with an energy-dispersive X-ray spectrometer (EDS). This verified the sample compositions based on the SC-XRD structure solutions.

Bond Valence Sums

Bond valence sums (BVS) calculations were undertaken for all compounds in this investigation using the parameters reported by Burns and co-workers[26] for U and all other atoms using those provided by Brese and O'Keeffe.[27]

Results and Discussion

Structural Studies (a) $K_2[UO_2(Mo_2O_7)_2]$

$K_2[UO_2(Mo_2O_7)_2]$ was found to adopt a layered monoclinic structure in space group $P2_1/c$ from measurements collected with SC-XRD. The unit cell was determined to be 652.79(7) Å^3 with a = 9.0775(5), b = 4.9444(2), c =15.2017(10) Å and β = 106.912(6)°. The structure of $K_2[UO_2(Mo_2O_7)_2]$ consists of UO_6 polyhedra with short axial oxo U-O bonds of length 1.773(6) Å characteristic of the uranyl group with hexavalent uranium.[28] Four longer U-O bonds are found in-plane of the UO_6 polyhedra with lengths ranging from 2.277(5) to 2.337(4) Å which are provide by MoO_6 polyhedra. Two crystallographic distinct MoO_6 polyhedra can be observed, $Mo(1)O_6$ and $Mo(2)O_6$, which

respectively have Mo-O bond lengths ranging from 1.679(5) to 2.135(4) Å and 1.743(4) to 2.283(5) Å. These MoO_6 polyhedra link together through an edge sharing motif to form two types of discrete Mo_2O_7 units that create a twin distorted zig-zag infinite chain motif parallel to the [010] direction, separating the UO_6 polyhedra to create $[UO_2(Mo_2O_7)_2]^{2-}$ layers (Figure 1d). Between these $[UO_2(Mo_2O_7)_2]^{2-}$ layers, charge stabilising K^+ cations can be found. Interestingly the arrangement the Mo_2O_7 units in $K_2[UO_2(Mo_2O_7)_2]$ particularly in linking isolated UO_2^{2+} moieties is reminiscent to that of related Bronzes and also of the structure of Brannerite.[29, 30] In classical uranyl molybdate compounds forming under more ambient pressure conditions, molybdate groups typically occur as isolated monomers that link UO_2^{2+} moieties as simple single bridges between them. In the case of $K_2[UO_2(Mo_2O_7)_2]$ the arrangement of Mo_2O_7 units is much more intricate and salient, requiring both a bridge between themselves via the twin distorted motif and also with their zig-zag arrangement. Such arrangements and central role to structure formation are more readily observed in that of described Bronzes and also of Brannerite of which $K_2[UO_2(Mo_2O_7)_2]$ is more closely resembled with, compared to more classical uranyl molybdates formed under ambient pressure conditions. [29, 30] Subsequently the occurrence of these Mo_2O_7 units in $K_2[UO_2(Mo_2O_7)_2]$ is suspected to be a consequence of the HT/HP conditions used in synthesis.

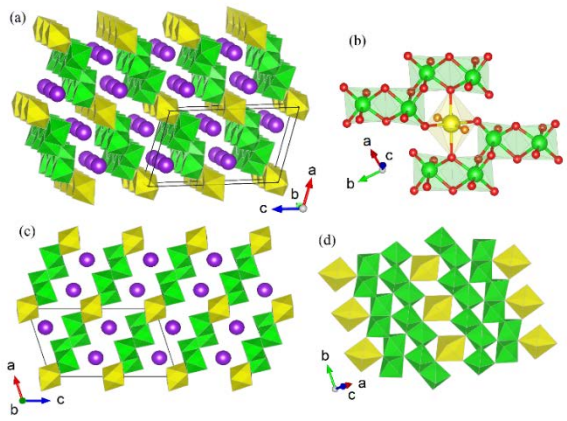

Figure 1. Structural representation of $K_2[UO_2(Mo_2O_7)_2]$ in (a) general view, (b) the coordination motif of the $[UO_2(Mo_2O_7)_2]^{2-}$ moiety, (c) [010] direction illustrating the layered structural motif, and (d) $[UO_2(Mo_2O_7)_2]$ layer connectivity. Note Yellow and green polyhedra respectively represent U(VI) and Mo(VI) polyhedra whereas the yellow, light green, purple, red and orange spheres respectively represent uranium, molybdenum, potassium, oxygen and uranyl oxygen atoms.

SEM/EDS measurements performed on crystals specimens of $K_2[UO_2(Mo_2O_7)_2]$ produced U:K:Mo ratios of 1.00:2.08:4.52 supporting the chemical formula assignment. BVS calculations for the U, Mo(1), Mo(2) and K^+ cations give values of 5.80, 6.03, 5.87 and 1.00 respectively indicating the as expected presence of U(VI), Mo(VI) and K(I). Full details crystallographic data can be found in Table 2, SEM results are given in supplementary information Figure S1a and Table S1a, bond lengths in supplementary information Table S3a, full BVS calculation results are presented in supplementary information Table S2a and structural representations presented in Figure 1 for $K_2[UO_2(Mo_2O_7)_2]$.

Table 2. Crystallographic data for all phases reported in this work

Compound	$K_2[UO_2(Mo_2O_7)_2]$	$K_2[(UO_2)_2(Mo(VI)_4Mo(IV)(OH)_2)O_{16}]$	$K_3[(UO_2)_6(OH)_2(MoO_4)_4(MoO_3OH)]$	$K_5[(UO_2)_{10}MoO_5O_{13}OH]\cdot H_2O$
Formula weight	955.99	696.53	2889.06	3263.74
Crystal system	Monoclinic	Triclinic	Orthorhombic	Triclinic
Space group	$P2_1/c$	$P\bar{1}$	*Pbcm*	*P*1
a (Å)	9.0775(5)	5.0468(9)	13.9807(12)	8.0728(5)
b (Å)	4.9444(2)	6.8982(7)	10.7427(9)	11.0224(7)
c (Å)	15.2017(10)	7.2414(12)	25.517(2)	11.4744(6)
α (°)	90	88.456(10)	90	111.118(6)
β (°)	106.912(6)	69.815(15)	90	102.845(5)
γ (°)	90	69.493(12)	90	104.506(6)
Unit cell Volume (Å^3)	652.79(7)	220.35(7)	3832.4(5)	865.09(11)
Z / *μ* (mm^{-1})	2/16.826	1/22.555	2/27.898	1/47.677
F(000)	852	305.5	4954.5	1353.0
d_{calcd} (g cm^{-3})	4.864	5.249	5.006	6.265
Rint	3.54	4.32	15.49	3.14
GOF	1.021	1.021	1.028	1.243
Final R_1 [a] [$I > 2\sigma(I)$]	0.0334	0.0430	0.0511	0.0340
Final wR_2 [b] [$I > 2\sigma(I)$]	0.0784	0.1055	0.0915	0.0827

Structural Studies (b) $K_2[(UO_2)_2(Mo(VI)_4Mo(IV)(OH)_2)O_{16}]$

$K_2[(UO_2)_2(Mo(VI)_4Mo(IV)(OH)_2)O_{16}]$ was found to adopt a disordered framework triclinic structure in space group $P\bar{1}$ from measurements collected with SC-XRD. The unit cell was determined to be 220.35(6) Å^3 with a = 5.0468(9), b = 6.8982(7), c = 7.2414(12) Å, α = 88.456(10), β = 69.815(15) and γ = 69.493(12)°. The structure of $K_2[(UO_2)_2(Mo(VI)_4Mo(IV)(OH)_2)O_{16}]$ consists of UO_6 polyhedra with short axial oxo U-O bonds of length 1.790(9) Å characteristic of the uranyl group with hexavalent uranium.[28] Four longer U-O bonds are found in-plane of the UO_6 polyhedra with lengths ranging from 2.277(10) to 2.300(7) Å which are provide by MoO_6 polyhedra that have Mo-O bond lengths ranging from 1.717(7) to 2.032(8) Å. These MoO_6 polyhedra coordinate to the uranyl group via corner sharing motif (Figure 2b) and when viewed from the [100] direction (Figure 2c) show an intersected layered motif of isolated uranyl groups connected via zig-zig Mo_2O_{10} units. A distinctive feature of $K_2[(UO_2)_2(Mo(VI)_4Mo(IV)(OH)_2)O_{16}]$ is the apparent occurrence of two different oxidation states of molybdenum, Mo(VI) and Mo(IV) from BVS and crystal chemical analysis. For the former variant typical aforementioned Mo-O lengths are well consistent with Mo(VI)[31] and BVS calculations support this with a value of 5.93. Whereas for the latter case, bond lengths of 1.869(2) to 2.1565(10) Å are determined which when BVS are calculated produce a value of 3.56 indicating the occurrence of Mo(IV). This is surprising result considering the use of

hexavalent MoO_3 in synthesis, nevertheless these deductions are based on BVS and crystal chemical analysis where spectroscopic measurements are required complete confirmation. Importantly these Mo(IV) polyhedra act to bridge the uranyl molybdate layers to form the framework structure (Figure 2c). It is suspect then the larger Mo(IV) cation better facilitates this than the smaller Mo(VI) cation which is likely a result of the HT/HP conditions used in synthesis.[32] The Mo(IV) cations form $Mo(IV)O_6$ polyhedra where four of these Mo-O bonds corner share with $Mo(VI)O_6$ polyhedra (Figure 2d) whereas the remaining two Mo-O bonds are found to be oxo and collinear (Figure 2c). The occurrence of oxo Mo-O oxygens for Mo(IV) in the given geometry in $K_2[(UO_2)_2(Mo(VI)_4Mo(IV)(OH)_2)O_{16}]$ is somewhat unusual, as although such Mo(IV) oxo bond occurrence have been observed readily in organometallic[33] and coordination complex[34] related systems its occurrence in a purely inorganic molybdate compound as that presented here is much less common. Nevertheless its occurrence is, as described, suspected to occur as a result of the HT/HP conditions used in synthesis. BVS calculations for these oxo Mo-O oxygens indicate the occurrence of OH^- groups (see supplementary information Table S2b). Interestingly the connectivity of these $Mo(IV)O_6$ units are found to be positionally disordered by charge balancing K^+ cations which partially substitute for the $Mo(IV)O_6$ units. The substitution motif is illustrated in Figure 2c and the average framework non-disordered structure in Figure 2a. For the vast majority of hexavalent uranyl group containing compounds, the structural motif adopted is that of infinite 2D layers or 1D chains due to the oxo-bonding nature of the uranyl group.[35] Uranyl containing framework structures can be found but more often these contain cation-cation interactions[1] (CCI's) via the uranyl groups or bridging oxyanion groups that facilitate the framework motif. In the case of $K_2[(UO_2)_2(Mo(VI)_4Mo(IV)(OH)_2)O_{16}]$, it does not contain uranyl group CCI's and forms a framework structure rather through connectivity of disordered $Mo(IV)O_6$ groups. However its formation and occurrence of positionally disordered $Mo(IV)O_6/K$ units is strongly speculated to be a result of the HT/HP conditions used in its synthesis.

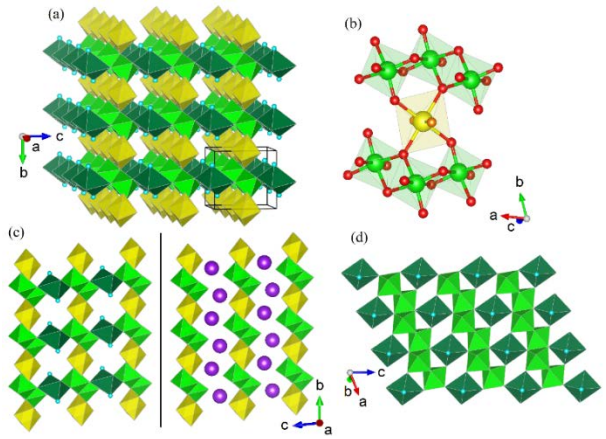

Figure 2. Structural representation of $K_2[(UO_2)_2(Mo(VI)_4Mo(IV)(OH)_2)O_{16}]$ in (a) general view (disordered K^+ cations have been omitted here), (b) highlighting the coordination motif about the UO_2^{2+} cation, (c) illustrating the structural variation between the disordered K^+ cations substituting for Mo(IV) units and (d) towards the [010] direction illustrating the connectivity motif between the Mo(VI) and Mo(IV) polyhedra. Note $Mo(VI)O_6$ and $Mo(IV)O_6$ polyhedra are presented by light and dark green respectively and aqua spheres represent OH^- group oxygens, hydrogens are not presented.

SEM/EDS measurements performed on crystals specimens of $K_2[(UO_2)_2(Mo(VI)_4Mo(IV)(OH)_2)O_{16}]$ produced U:K:Mo ratios of 1.00:1.39;1.93 supporting the chemical formula assignment. BVS calculations for the U, Mo(1), Mo(2) and K^+ cations give values of 6.14, 5.65, 3.56 and 0.96 respectively indicating the presence of U(VI), Mo(VI), Mo(IV) and K(I). Full details crystallographic data can be found in Table 2, SEM results are given in supplementary information Figure S1b and Table S1b, bond lengths in supplementary information Table S3b, full BVS calculation result are given in supplementary information Table S2b and structural representations presented in Figure 2 for $K_2[(UO_2)_2(Mo(VI)_4Mo(IV)(OH)_2)O_{16}]$.

Structural Studies (c) $K_3[(UO_2)_6(OH)_2(MoO_4)_6(MoO_3OH)]$

$K_3[(UO_2)_6(OH)_2(MoO_4)_6(MoO_3OH)]$ was found to adopt a disordered framework orthorhombic structure in space group *Pbcm*. The unit cell was determined to be 3832.4(5) $Å^3$ with a = 13.9807(12), b = 10.7427(9) and c = 25.517 Å. The structure of $K_3[(UO_2)_6(OH)_2(MoO_4)_6(MoO_3OH)]$ consists of a series of small tubular channels and large elliptically-shaped cavities constructed from interconnected UO_7 and MoO_4 polyhedra (Figure 3). The UO_7 polyhedra contain short axial oxo U-O bonds with length ranging from 1.708(16) to 1.782(11) Å characteristic of the uranyl group with hexavalent uranium.[28] The equatorial U-O bond length are found to range from 2.317(11) to 2.582(15) Å, where in the cases of U(3) and U(4) a significantly longer length of 2.566(14) and 2.582(15) Å is observed respectively, which is attributed to the presence of OH^- groups. The MoO_4 units contain Mo-O bond lengths ranging from 1.745(11) to 1.781(10) Å. The small tubular channels can be observed to run parallel to the [010] direction where they contain charge balancing K^+ cations that are coordinated by UO_7 polyhedra bridged by MoO_4 through a corner share motif to form $[UO_2(MoO_4)_5]^{8-}$ units (Figure 3c and 4). The larger elliptically-shaped cavities also contain charge balancing K^+ cations but instead are found to be disordered (Figure 4). The disordering is attributed to the topology of the cavities coupled with the presence of OH^- groups extending from the UO_7 polyhedra forming $[UO_2(MoO_4)_4OH]^{7-}$ moieties that coordinate to the K^+ cations (Figure 4).

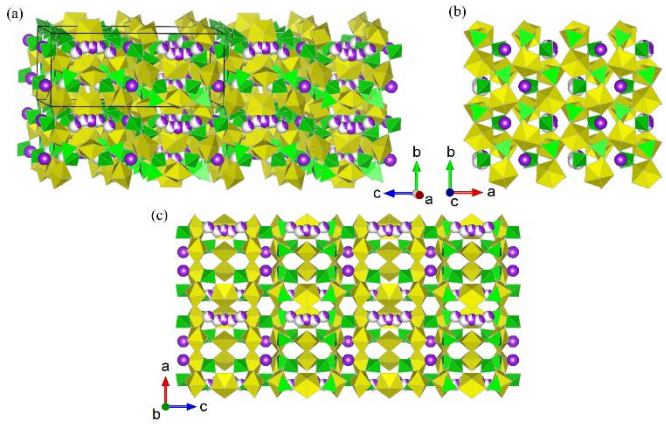

Figure 3. Structural representation $K_3[(UO_2)_6(OH)_2(MoO_4)_6(MoO_3OH)]$ in (a) general view, (b) the [001] direction, and (c) toward the [010] direction. Disordered K^+ cations are represented by partially shaded purple spheres. Note OH^- groups have been omitted for clarity.

SEM/EDS measurements performed on crystals specimens of $K_3[(UO_2)_6(OH)_2(MoO_4)_6(MoO_3OH)]$ produced U:K:Mo ratios of 1.00:0.47:1.30 supporting the chemical formula assignment. BVS calculations for the U(1), U(2), U(3), U(4), Mo(1), Mo(2), Mo(3), Mo(4), K(1), K(2), K(3) and K(4) cations give values of 6.11, 6.04, 6.17, 6.21, 6.08, 5.96. 6.00, 6.06, 0.70, 0.78, 0.99 and 0.60 respectively indicating the as expected presence of U(VI), Mo(VI) and K(I). Full details crystallographic data can be found in Table 2, SEM results are given in supplementary information Figure S1c and Table S1c, bond lengths in supplementary information Table S3c, full BVS calculation results are presented in supplementary information Table S2c and structural representations presented in Figure 3 and 4 for $K_3[(UO_2)_6(OH)_2(MoO_4)_6(MoO_3OH)]$.

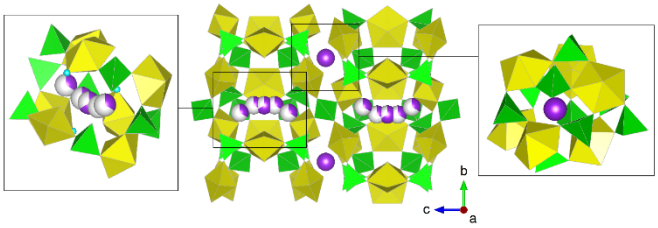

Figure 4. Structural representation of $K_3[(UO_2)_6(OH)_2(MoO_4)_6(MoO_3OH)]$ highlighting the coordination environment of the disordered K^+ cations (left) within the larger OH^- group possessing void space and the ordered K^+ cations (right) within the smaller OH^- absent void space. Note OH^- group possessing oxygens have been marked as aqua spheres, hydrogens not shown.

Structural Studies (d) $K_5[(UO_2)_{10}MoO_5O_{11}OH]\cdot H_2O$

$K_5[(UO_2)_{10}MoO_5O_{11}OH]\cdot H_2O$ was found to adopt a triclinic framework structure in space group $P\bar{1}$. The unit cell was determined to be 865.09(10) $Å^3$ with a = 8.0728(5), b = 11.0224(7), c = 11.4744(6) Å, α = 111.118(6), β = 102.845(5) and γ = 104.506(6) °. The structure of $K_5[(UO_2)_{10}MoO_5O_{11}OH]\cdot H_2O$ consists of a mixture of UO_6, hexagonal, and UO_7, pentagonal, bipyramid polyhedra and also MoO_5 polyhedra which connect through edge and corner sharing motifs to form the network structure. The structure consists of large tubular channels that run parallel to the [001] direction of which they are perforated by triangular and hexagonal like voids (Figure 5). Within the channels, disordered charge balancing K^+ cations an OH^- group and H_2O molecules can be found. Compared to the network structure of $K_3[(UO_2)_6(OH)_2(MoO_4)_6(MoO_3OH)]$ where the charge balancing disordered K^+ cations are essentially contained in the closed voids, the channels of $K_5[(UO_2)_{10}MoO_5O_{11}OH]\cdot H_2O$ are open. The UO_6 and UO_7 polyhedra both possess short axial oxo U-O bonds that range from 1.71(4) to 1.98(3) Å. Whereas longer U-O bonds are found in-plane of both UO_6 and UO_7 polyhedra that range from 2.15(4) to 2.52(4) Å. Although the shorter axial oxo U-O bonds are relatively longer than those described in the aforementioned structures in this investigation, they are still consistent with the presence of the uranyl group with hexavalent uranium.[16, 23, 35] The MoO_5 polyhedra possess a single in-plane Mo-O bond of length 1.67(4) Å. Opposite and collinear to this Mo-O bond a H_2O oxygen can be found at distance of 2.68(4) Å. The MoO_5 polyhedra link with UO_7 polyhedra parallel to the [001] direction (Figure 5c).

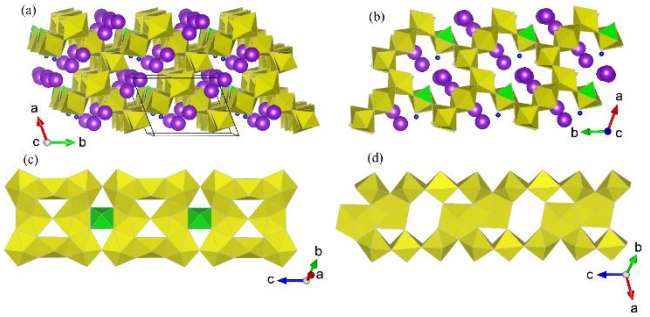

Figure 5. Structural representation of $K_5[(UO_2)_{10}MoO_5O_{11}OH]\cdot H_2O$ (a) general view, (b) towards the [001] direction, (c) and (d) respectively highlighting the connectivity of the uranyl and molybdate polyhedra that form channels within $K_5[(UO_2)_{10}MoO_5O_{11}OH]\cdot H_2O$. Note small blue spheres represent H_2O oxygen atoms, hydrogens are not shown.

A distinctive feature of the structure of $K_5[(UO_2)_{10}MoO_5O_{11}OH]\cdot H_2O$ is the presence of CCIs between the UO_6 and UO_7 polyhedra (Figure 6). As described previously, hexavalent uranyl containing compounds typically form layered structures due to the oxo bonding motif of the axial uranyl oxygens. Exceptions to this occur when other metal polyhedra species are present to bridge layers, for instance the bridging $Mo(IV)O_6$ polyhedra in $K_2[(UO_2)_2(Mo(VI)_4Mo(IV)(OH)_2)O_{16}]$, or through CCIs, these allow for the potential occurrence of framework structure to form. In the case of $K_5[(UO_2)_{10}MoO_5O_{11}OH]\cdot H_2O$ the CCIs arise from uranyl groups in the UO_6 and UO_7 polyhedra (Figure 6). Although CCI interactions have been described differently in inorganic science[36, 37] we describe those observed in $K_5[(UO_2)_{10}MoO_5O_{11}OH]\cdot H_2O$ using the notation by Alekseev *et al.*[1] where it can be classified as a type VI. This coordination motif and geometry of the CCI is a result of the interaction between the UO_6 into the UO_7 polyhedra.

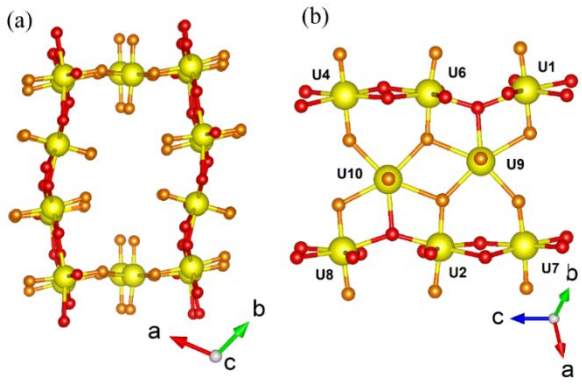

Figure 6. Representation of the cation-cation interactions that occur in $K_5[(UO_2)_{10}MoO_5O_{11}OH]\cdot H_2O$ between the uranyl groups that allow for the formation of the (a) channel structure and (b) the specific CCI motif adopted. Note yellow, red and orange spheres respectively represent uranium, oxygen and uranyl oxygen atoms.

SEM/EDS measurements performed on crystals specimens of $K_5[(UO_2)_{10}MoO_5O_{11}OH]\cdot H_2O$ produced U:K:Mo ratios of 1.00:0.54:0.13 supporting the chemical formula assignment. Full BVS calculations

for $K_5[(UO_2)_{10}MoO_5O_{11}OH]\cdot H_2O$ can be found in supplementary information Table S2d of which the assignment of U(VI), Mo(VI), K(I) and the presence of a H_2O molecule and an OH^- group is supported. Full details crystallographic data can be found in Table 2, SEM results are giving in supplementary information Figure S1d and Table S1d, bond lengths in supplementary information Table S3d, full BVS calculation results are presented in supplementary information Table S2d and structural representations presented in Figure 5 and 6 for $K_5[(UO_2)_{10}MoO_5O_{11}OH]\cdot H_2O$.

Structural and Chemical Trends in the A^+-U(VI)-Mo-O System

With respect to literature, the uranyl molybdate compounds uncovered in this investigation are apparently the first to be synthesised and characterised from HT/HP conditions. A plethora of uranyl molybdate compounds are known, particularly through the pioneering studies of Krivovichev and Burns, although these have been near solely obtained via either high temperature solid state or hydrothermal synthesis methods. Accordingly it is pertinent to compare and contrast the structural-chemical trends that occur between the compounds uncovered in this investigation with previous literature. The number of well characterised reported uranyl molybdates extends over 100 compounds,[38] many of these are outside of the scope of the current investigation and thus the following discussion will focus on the quaternary A^+-U(VI)-Mo-O system (A are alkali metal cations) of which the novel structures uncovered in this investigation are a part of. Table 3 summarises the present knowledge of these reported phases, their structural and chemical trends along with the novel structures reported in this investigation obtained through HT/HP synthesis methods.

When Table 3 is inspected, the synthesis technique, specifically the level of pressure applied, and the ratio of uranium and molybdenum units, appear to be key parameters which dictate the structural chemistry of as synthesised uranyl molybdates. For structures obtained from high temperature conditions – low pressure conditions (0.1 MPa) largely a mix of 0D cluster, 1D chains and 2D layered structures with some 3D frameworks are reported. In contrast under hydrothermal conditions (mid pressure range of 2-20 MPa), they are a combination of 2D layered or 3D frameworks whereas from HT/HP (up to 4 GPa) conditions the structures are predominantly 3D frameworks. This trend is further apparent when graphically illustrated as shown in Figure 7 which, derived from the values given in Table 3, plots the ratio of U/Mo against the structural dimensionality for specific synthesis methods used with their relative occurrence. Although there is paucity of information for uranyl molybdates obtained from HT/HP conditions, outside of the present investigation, the described trend of pressure leading to higher dimensional structure formation from Table 3 and Figure 7 is consistent with previous systematic investigations of uranium nickel oxides, uranyl borates[39] and also thorium molybdates under HT/HP conditions.[20, 23]

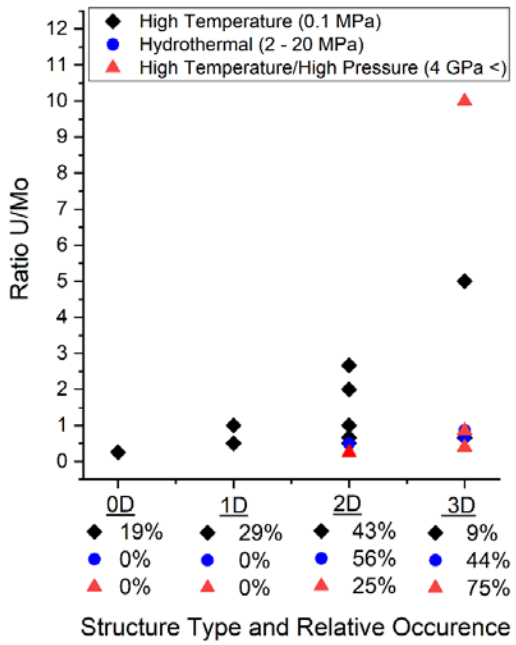

Figure 7. Comparison of (top) $K_5[(UO_2)_{10}MoO_5O_{11}OH]\cdot H_2O$ and (bottom) $Li_4[(UO_2)_{10}O_{10}(Mo_2O_8)]$.[1] Pink spheres represent Li^+ in $Li_4[(UO_2)_{10}O_{10}(Mo_2O_8)]$.

The apparent increase in structural dimensionality in the A^+-U(VI)-Mo-O system with increasing pressure, as shown by the trends in Table 3 and Figure 7, is argued to be further related to the U/Mo ratio. The ability for uranyl 3D framework structures to form is often facilitated via bridging coordinating ligands or through CCIs, which as mentioned, are relatively rare for hexavalent uranyl groups due to unfavourable electrostatic interactions which are less pronounced in lower valent uranium compounds.[35] Consequently uranyl containing compounds tend to form lower dimensional 1D chain or 2D layered structures which minimise these interactions, rather than 3D frameworks when sufficient bridging ligands are not available. Consequently synthesis techniques for higher dimensional hexavalent uranyl compounds often use excess additions of bridging oxyanion ligands for instance in $Cs_2[(UO_2)(Ge_2O_6)]\cdot H_2O$[40] and $K_2[(UO_2)_2(VO)_2(IO_6)_2O]\cdot H_2O$[41] or organic bridging units for instance in uranium molecular organic framework (MOF) synthesis[42] relative to uranium to drive 3D structure formation. However, in the case of molybdenum a delicate balance is necessary between the ratio of uranium units and bridging molybdate ligands for 3D framework structure formation. If the relative ratio of uranium to molybdenum is too low under ambient pressure conditions (i.e U/Mo $\leq$ 1/2) from Table 3 and Figure 7 there is tendency for 0D clusters and 1D chain structures to form. For example the 0D cluster structures for $A_6[(UO_2)(MoO_4)_4]$[31, 43, 44] A = Na, Rb and Cs, when U/Mo = 1:4 or the 1D chain structures for $A_6[(UO_2)_2O(MoO_4)_4]$[31, 44] A = Na, K and Rb, when U/Mo = 1:2. This observation is somewhat unsurprising as such a strategy involving relative high additions of molybdenum relative to metal units is often employed in the synthesis of novel 0D cluster molybdate containing polyoxometalate (POMs) compounds.[45] If the relative amount of uranium to molybdenum is reduced, this can assist in increasing the dimensionality of structures as for example can be seen in $Rb_6[(UO_2)(MoO_4)_4]$, $Rb_2[(UO_2)(MoO_4)_2]$ and

$Rb_2[(UO_2)_2(MoO_4)_3]$ which were all synthesised under the same high temperature conditions by Krivovichev and Burns[44] but show a respective transition from 0D cluster, 2D layer to 3D framework structures with increasing U/Mo ratio (1:4, 1:2, 2:3).

When Table 3 and Figure 7 are considered it is argued that the introduction of pressure during synthesis can aid in increasing dimensionality of structure formation through the condensation of polyhedra.[46] This can be observed when comparing the 2D layered structure of $K_2[UO_2(Mo_2O_7)_2]$ obtained from HT/HP conditions with the 0D cluster structures of $A_6[(UO_2)(MoO_4)_4]$ *A* = Na, Rb and Cs, in which the different variants possess the same ratio of U to Mo units (1:4).[31, 43, 44] However a pertinent difference is the occurrence Mo_2O_7 dimers which link with other Mo_2O_7 dimers and uranyl units to create the layered structure of $K_2[UO_2(Mo_2O_7)_2]$. Although MoO_3 as reagent is used in both syntheses of $K_2[UO_2(Mo_2O_7)_2]$ and $A_6[(UO_2)(MoO_4)_4]$ *A* = Na, Rb and Cs[31, 43, 44], the use of pressure conditions in the former structures synthesis has likely driven the condensation and oligomerization of molybdenum units forming the Mo_2O_7 dimers. Such suspected oligomerization via pressure is consistent with previous *in situ* studies such as for and $KDy(MoO_4)$ and $KY(MoO_4)$.[47] similar observations have also been made in uranyl borate studies utilizing HT/HP conditions, where the occurrence of unique higher dimensionality structures have been found.[39] Indeed a common theme of the structures obtained from this investigation using HT/HP conditions is the common occurrence of molybdate oligomers, disordered counter cations and higher dimensional structures, which are apparently far less encountered in structures obtained from high temperature and hydrothermal conditions.

Table 3. Comparison of reported structures for the A^+-U(VI)-Mo-O system (A^+ = alkali metal cations)

Synthesis Conditions	Compound	Ratio U/Mo	Structural Motif	Mo-O Oligomer Type	Structure Type/ Space Group	Reference
High Temperature Synthesis	β-$Cs_2[(UO_2)_2(MoO_4)_3]$	2:3	2D layered	MoO_4	Tetragonal/ $P4_2/n$	Krivovichev *et al.*[48]
	$Cs_2[(UO_2)O(MoO_4)]$	1:1	1D Chains	MoO_4	Orthorhombic/ $Pca2_1$	Alekseev *et al.*[49]
	$Li_2[(UO_2)(MoO_4)_2]$	1:2	1D Chains	MoO_4	Triclinic/ $P\bar{1}$	Krivovichev and Burns[50]
	$Na_2[(UO_2)(MoO_4)_2]$	1:2	2D Layered	MoO_4	Orthorhombic/ $P2_12_12_1$	Krivovichev *et al.*[51]
	$K_2[(UO_2)(MoO_4)_2]$	1:2	2D Layered	MoO_4	Monoclinic/ $P2_1/c$	Sadikov *et al.*[52]
	$Rb_2[(UO_2)(MoO_4)_2]$	1:2	2D Layered	MoO_4	Monoclinic/ $P2_1/c$	Krivovichev and Burns[44]
	$Cs_2[(UO_2)(MoO_4)_2]$	1:2	2D layered	MoO_4	Orthorhombic/ *Pbcn*	Krivovichev and Burns[53]
	$Rb_2[(UO_2)_2(MoO_4)_3]$	2:3	3D Framework	MoO_4	Orthorhombic/ $Pna2_1$	Krivovichev and Burns[44]
	$K_2[UO_2)_2O_2(MoO_4)]$	2:1	2D Layered	MoO_4	Monoclinic/ $P2_1/c$	Obbade *et al.*[54]
	$Rb_2[(UO_2)_2O_2(MoO_4)]$	2:1	2D Layered	MoO_4	Monoclinic/ $P2_1/c$	Alekseev *et al.*[55]
High Temperature Synthesis	$Cs_4[(UO_2)_3O(MoO_4)_2(MoO_5)]$	1:1	2D Layered	MoO_4, MoO_5	Triclinic/ *P*1	Krivovichev and Burns[43]
	$Li_4[(UO_2)_{10}O_{10}(Mo_2O_8)]$	5:1	3D Framework	Mo_2O_8	Monoclinic/ $P2_1/c$	Alekseev *et al.*[1]
	$Na_6[(UO_2)(MoO_4)_4]$	1:4	0D Clusters	MoO_4	Triclinic/ $P\bar{1}$	Krivovichev and Burns[31]
	$Rb_6[(UO_2)(MoO_4)_4]$	1:4	0D Clusters	MoO_4	Monoclinic/ C2/c	Krivovichev and Burns[44]
	$Cs_6[(UO_2)(MoO_4)_4]$	1:4	0D Clusters	MoO_4	Triclinic/ $P\bar{1}$	Krivovichev and Burns[43]
	$Na_6[(UO_2)_2O(MoO_4)_4]$	1:2	1D Chains	MoO_4	Triclinic/ $P\bar{1}$	Krivovichev and Burns[31]
	$K_6[(UO_2)_2O(MoO_4)_4]$	1:2	1D Chains	MoO_4	Triclinic/ $P\bar{1}$	Krivovichev and Burns[31]
	$Rb_6[(UO_2)_2O(MoO_4)_4]$	1:2	1D Chains	MoO_4	Triclinic/ $P\bar{1}$	Krivovichev and Burns[44]
	$Cs_6[(UO_2)_2(MoO_4)_3(MoO_5)]$	1:2	1D Chains	MoO_5	Triclinic/ $P\bar{1}$	Yagoubi *et al.*[56]
	$K_8[(UO_2)_8O_6(MoO_5)_3]$	8:3	2D Layered	MoO_5	Tetragonal/*P*4/n	Obbade *et al.*[54]
Hydrothermal	α-$Cs_2[(UO_2)_2(MoO_4)_3]$	2:3	3D Framework	MoO_4	Orthorhombic/ $Pna2_1$	Krivovichev *et al.*[48]
	$Na_2[(UO_2)(MoO_4)_2]\cdot 4H_2O$	1:2	2D layered	MoO_4	Monoclinic/ $P2_1/n$	Krivovichev and Burns[57]
	$K_2[(UO_2)(MoO_4)_2]\cdot H_2O$	1:2	2D Layered	MoO_4	Monoclinic/ $P2_1/c$	Krivovichev *et al.*[51]
	$Rb_2[(UO_2)(MoO_4)_2]\cdot H_2O$	1:2	2D layered	MoO_4	Monoclinic/ $P2_1/c$	Khrustalev *et al.*[58]
	$(NH_4)_2[(UO_2)(MoO_4)_2]\cdot H_2O$	1:2	2D layered	MoO_4	Monoclinic/ $P2_1/c$	Andreev *et al.*[59]

	$Cs_2[(UO_2)(MoO_4)_2]\cdot H_2O$	1:2	2D layered	MoO_4	Monoclinic/ $P2_1/c$	Krivovichev and Burns[53]
	$Rb_2[(UO_2)_6(MoO_4)_7]\cdot 2H_2O$	6:7	3D Framework	MoO_4	Orthorhombic/ *Pbcn*	Krivovichev and Burns[44]
	$(NH_4)_2[(UO_2)_6(MoO_4)_7]\cdot 2H_2O$	6:7	3D Framework	MoO_4	Orthorhombic/ *Pbcm*	Krivovichev and Burns[60]
	$Cs_2[(UO_2)_6(MoO_4)_7]\cdot 2H_2O$	6:7	3D Framework	MoO_4	Orthorhombic/ *Pbcm*	Krivovichev and Burns[60]
High Pressure/High Temperature	$K_2[UO_2(Mo_2O_7)_2]$	1:4	2D layered	Mo_2O_7	Monoclinic/ $P2_1/c$	Present Investigation
	$K_2[(UO_2)_2(Mo(VI)_4Mo(IV)(OH)_2)O_{16}]$	2:5	3D Framework	$Mo_5O_{16}(OH)_2$	Triclinic/ $P\bar{1}$	Present Investigation
	$K_3[(UO_2)_6(OH)_2(MoO_4)_6(MoO_3OH)]$	6:7	3D Framework	MoO_4	Orthorhombic/ *Pbcm*	Present Investigation
	$K_5[(UO_2)_{10}MoO_5O_{11}OH]\cdot H_2O$	10:1	3D Framework	MoO_5	Triclinic/ $P\bar{1}$	Present Investigation

$Li_4[(UO_2)_{10}O_{10}(Mo_2O_8)]$ is somewhat of an exception to the described structural trends occurring in Table 3 forming a 3D framework structure under high temperature conditions and possessing Mo_2O_8 dimers with a large ratio of U/Mo. A pertinent aspect of this structure is the occurrence of CCIs that allow for the framework structure to occur. $Li_4[(UO_2)_{10}O_{10}(Mo_2O_8)]$ is strikingly similar to $K_5[(UO_2)_{10}MoO_5O_{11}OH]\cdot H_2O$, both structures contain open channels where charge balancing A^+ cations are contained as shown comparatively in Figure 8 and further both possess the same CCI connectivity motif between the uranyl groups. Distinction is made in $K_5[(UO_2)_{10}MoO_5O_{11}OH]\cdot H_2O$ which contains disordered K^+ and H_2O molecules within the channels compared to the ordered Li^+ in the channels of $Li_4[(UO_2)_{10}O_{10}(Mo_2O_8)]$. The disordering, which is also seen in $K_2[(UO_2)_2(Mo(VI)_4Mo(IV)(OH)_2)O_{16}]$ and $K_3[(UO_2)_6(OH)_2(MoO_4)_6(MoO_3OH)]$ with respect to molybdate and K^+ cations respectively, is argued a result of the HT/HP conditions used in the synthesis. Furthermore the ratio of U/Mo in $K_5[(UO_2)_{10}MoO_5O_{11}OH]\cdot H_2O$ compared to $Li_4[(UO_2)_{10}O_{10}(Mo_2O_8)]$ is larger in the former compound with 10:1 compared to 5:1 respectively. This is also argued a result of the HT/HP conditions used were the addition of pressure is driving an increase in concentration of uranium polyhedra present via their condensation. Such behaviour is consistent and reminiscent with that observed in the higher pressure form of $NiUO_4$, α, which possess more regularly connected UO_6 polyhedra compared to its lower pressure β form.[23]

It is known that HT/HP conditions provide a means to which unique topologies and structural chemistry can be accessed that are rarely encountered in more mild and ambient pressure based synthesis methods.[61] The structures uncovered in this investigation, namely $K_2[UO_2(Mo_2O_7)_2]$, $K_2[(UO_2)_2(Mo(VI)_4Mo(IV)(OH)_2)O_{16}]$, $K_3[(UO_2)_6(OH)_2(MoO_4)_6(MoO_3OH)]$ and $K_5[(UO_2)_{10}MoO_5O_{11}OH]\cdot H_2O$, exemplify this statement possessing structural chemistry that is far more exotic compared to their extended A^+-U(VI)-Mo-O family of structures. Pertinently the previous structures investigated were confined to high temperature and hydrothermal methods which resulted in largely low dimensional monomeric molybdate based structures. The application of HT/HP conditions is argued to drive and favour structure formation towards potassium uranyl molybdate compounds with higher dimensionality and more diverse structural chemistry with respect to the occurrence of cation disorder, diverse molybdate oligomer occurrence and potential CCIs. Prior to this investigation there were no apparent reports of uranyl molybdates being synthesised from HT/HP conditions. That the use of consistent HT/HP conditions with only subtle change to reagent addition has resulted in such diverse production of unique structures, it can considered that this investigation is only the tip-of-iceberg in uranyl molybdate HT/HP synthesis and unique structural design. By utilizing identified structural trends from this investigation such as through targeted usage of metal to molybdenum ratios with the consideration of applied pressure, it may guide associated functional material design and synthesis efforts such as for POM framework generation in exchange and separation applications.[45]

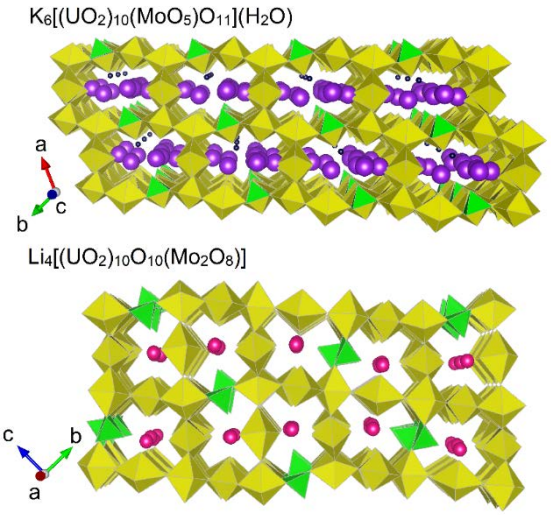

Figure 8. Ratio of U/Mo against the structural dimensionality for specific synthesis methods in structures a part of the A^+-U(VI)-Mo-O system (A = alkali metal cations) from Table 8. The relative occurrence of each structure type from synthesis is given below the x-axis.

Conclusion

In summary, we have synthesised the first examples of uranyl molybdate compounds from HT/HP synthesis conditions, namely $K_2[UO_2(Mo_2O_7)_2]$, $K_2[(UO_2)_2(Mo(VI)_4Mo(IV)(OH)_2)O_{16}]$, $K_3[(UO_2)_6(OH)_2(MoO_4)_6(MoO_3OH)]$ and $K_5[(UO_2)_{10}MoO_5O_{11}OH]\cdot H_2O$, and characterised them using single crystal X-ray diffraction data and SEM/EDS microscopy. By comparing these compounds within the broader family of A^+-U(VI)-Mo-O variants from literature, we have identified the key role pressure and the ratio of U/Mo units have in dictating the structural dimensionality of resulting structures during

synthesis. By increasing the amount of pressure present during synthesis, structures that would otherwise likely occur as low dimensional uranyl monomeric molybdate compounds which favour low ratios of U/Mo units in ambient pressure conditions are argued to be driven towards higher dimensional structures with larger U/Mo ratios via condensation of polyhedra resulting in the increasing likelihood of oligomerization of molybdate units. Similar observations have been made in nickel uranium oxides,[23] thorium molybdates[20] among other well-known examples in organic and inorganic related studies,[62, 63] but this is apparently the first systematic structural-chemical study for uranyl molybdate system. Consequently, this discussion provides a road map for which specific structural dimensionalities and functional groups in uranyl molybdates can be accessed and controlled via appropriate consideration of applied pressure.

Acknowledgements

The work has been supported by the Deutsche Forschungsgemeinschaf (DFG) grant AL1527/3-1. S. Wang acknowledge funding support from National Natural Science Foundation of China (21761132019).

Notes and references

1. E. V. Alekseev, S. V. Krivovichev, T. Malcherek and W. Depmeier, *Inorg. Chem.*, 2007, **46**, 8442-8444.
2. A. P. V. Soares and M. F. Portela, *Catal. Rev.-Sci. Eng.*, 2005, **47**, 125-174.
3. T. T. Basiev, A. A. Sobol, Y. K. Voronko and P. G. Zverev, *Optical Materials*, 2000, **15**, 205-216.
4. L. Malavasi, C. A. J. Fisher and M. S. Islam, *Chem. Soc. Rev.*, 2010, **39**, 4370-4387.
5. C. Lind, D. G. VanDerveer, A. P. Wilkinson, J. H. Chen, M. T. Vaughan and D. J. Weidner, *Chemistry of Materials*, 2001, **13**, 487-490.
6. D. Christofilos, G. Kourouklis and S. Ves, *J. Phys. Chem. Solids*, 1995, **56**, 1125-1129.
7. W. Paraguassu, M. Maczka, A. Souza Filho, P. Freire, J. Mendes Filho, F. Melo, L. Macalik, L. Gerward, J. S. Olsen and A. Waskowska, *Physical Review B*, 2004, **69**, 094111.
8. V. Dmitriev, V. Sinitsyn, R. Dilanian, D. Machon, A. Kuznetsov, E. Ponyatovsky, G. Lucazeau and H. P. Weber, *J. Phys. Chem. Solids*, 2003, **64**, 307-312.
9. H. Kahari, M. Teirikangas, J. Juuti and H. Jantunen, *J. Am. Ceram. Soc.*, 2014, **97**, 3378-3379.
10. H. Kleykamp, *J. Nucl. Mater.*, 1985, **131**, 221-246.
11. E. C. Buck, D. J. Wronkiewicz, P. A. Finn and J. K. Bates, *J. Nucl. Mater.*, 1997, **249**, 70-76.
12. J. N. Cross, P. M. Duncan, E. M. Villa, M. J. Polinski, J.-M. Babo, E. V. Alekseev, C. H. Booth and T. E. Albrecht-Schmitt, *Journal of the American Chemical Society*, 2013, **135**, 2769-2775.
13. N. D. Dahale, M. Keskar and K. D. Singh Mudher, *J. Alloy. Compd.*, 2006, **415**, 244-250.
14. B. Xiao, M. Klinkenberg, D. Bosbach, E. V. Suleimanov and E. V. Alekseev, *Inorg. Chem.*, 2015, **54**, 5981-5990.
15. J. Lin, Q. Liu, Z. Yue, K. Diefenbach, L. Cheng, Y. Lin and J.-Q. Wang, *Dalton Trans.*, 2019, **48**, 4823-4829.
16. G. Murphy, B. J. Kennedy, B. Johannessen, J. A. Kimpton, M. Avdeev, C. S. Griffith, G. J. Thorogood and Z. M. Zhang, *J. Solid State Chem.*, 2016, **237**, 86-92.
17. G. L. Murphy, B. J. Kennedy, J. A. Kimpton, Q. Gu, B. Johannessen, G. Beridze, P. M. Kowalski, D. Bosbach, M. Avdeev and Z. Zhang, *Inorg. Chem.*, 2016, **55**, 9329-9334.
18. G. L. Murphy, C. H. Wang, Z. M. Zhang, P. M. Kowalski, G. Beridze, M. Avdeev, O. Muransky, H. E. A. Brand, Q. F. Gu and B. J. Kennedy, *Inorg. Chem.*, 2019, **58**, 6143-6154.
19. G. L. Murphy, C.-H. Wang, G. Beridze, Z. Zhang, J. A. Kimpton, M. Avdeev, P. M. Kowalski and B. J. Kennedy, *Inorg. Chem.*, 2018, **57**, 5948-5958.
20. B. Xiao, P. Kegler, T. M. Gesing, L. Robben, A. Blanca-Romero, P. M. Kowalski, Y. Li, V. Klepov, D. Bosbach and E. V. Alekseev, *Chemistry – A European Journal*, 2016, **22**, 946-958.
21. G. L. Murphy, E. M. Langer, O. Walter, Y. Wang, S. Wang and E. V. Alekseev, *Inorg. Chem.*, 2020, **59**, 7204-7215.
22. H. H. Osman, P. Pertierra, M. A. Salvadó, F. Izquierdo-Ruiz and J. M. Recio, *Physical Chemistry Chemical Physics*, 2016, **18**, 18398-18405.
23. G. L. Murphy, P. Kegler, Y. Zhang, Z. Zhang, E. V. Alekseev, M. D. de Jonge and B. J. Kennedy, *Inorg. Chem.*, 2018, **57**, 13847-13858.
24. G. Sheldrick, *Acta Crystallographica Section A*, 2008, **64**, 112-122.
25. A. Spek, *J. Appl. Crystallogr.*, 2003, **36**, 7-13.
26. P. C. Burns, R. C. Ewing and F. C. Hawthorne, *Can. Mineral.*, 1997, **35**, 1551-1570.

27. N. E. Brese and M. O'Keeffe, *Acta Crystallographica Section B*, 1991, **47**, 192-197.
28. P. C. Burns, *Can. Mineral.*, 2005, **43**, 1839-1894.
29. J. Graham and A. Wadsley, *Acta Crystallographica*, 1966, **20**, 93-100.
30. R. Ruh and A. Wadsley, *Acta Crystallographica*, 1966, **21**, 974-978.
31. S. V. Krivovichev and P. C. Burns, *The Canadian Mineralogist*, 2001, **39**, 197-206.
32. R. Shannon, *Acta Crystallographica Section A*, 1976, **32**, 751-767.
33. P. Legzdins, E. C. Phillips and L. Sanchez, *Organometallics*, 1989, **8**, 940-949.
34. I. W. Boyd and J. T. Spence, *Inorg. Chem.*, 1982, **21**, 1602-1606.
35. G. L. Murphy, Z. Zhang and B. J. Kennedy, in *Complex Oxides: An Introduction*, 2019, pp. 103-130.
36. B. Vlaisavljevich, P. Miró, D. Ma, G. E. Sigmon, P. C. Burns, C. J. Cramer and L. Gagliardi, *Chemistry – A European Journal*, 2013, **19**, 2937-2941.
37. J. B. Goodenough, *Physical Review*, 1960, **117**, 1442-1451.
38. C. R. Groom, I. J. Bruno, M. P. Lightfoot and S. C. Ward, *Acta Crystallographica Section B*, 2016, **72**, 171-179.
39. S. Wu, S. Wang, M. Polinski, O. Beermann, P. Kegler, T. Malcherek, A. Holzheid, W. Depmeier, D. Bosbach, T. E. Albrecht-Schmitt and E. V. Alekseev, *Inorg. Chem.*, 2013, **52**, 5110-5118.
40. J. Ling, J. M. Morrison, M. Ward, K. Poinsatte-Jones and P. C. Burns, *Inorg. Chem.*, 2010, **49**, 7123-7128.
41. R. E. Sykora and T. E. Albrecht-Schmitt, *Inorg. Chem.*, 2003, **42**, 2179-2181.
42. P. Li, N. A. Vermeulen, X. Gong, C. D. Malliakas, J. F. Stoddart, J. T. Hupp and O. K. Farha, *Angewandte Chemie International Edition*, 2016, **55**, 10358-10362.
43. S. V. Krivovichev and P. C. Burns, *The Canadian Mineralogist*, 2002, **40**, 201-209.
44. S. V. Krivovichev and P. C. Burns, *J. Solid State Chem.*, 2002, **168**, 245-258.
45. L. Vilà-Nadal and L. Cronin, *Nature Reviews Materials*, 2017, **2**, 17054.
46. O. Shameema and E. D. Jemmis, *Angewandte Chemie International Edition*, 2008, **47**, 5561-5564.
47. A. Jayaraman, S. Sharma, S. Wang, S. Shieh, L. Ming and S. W. Cheong, *Journal of Raman spectroscopy*, 1996, **27**, 485-490.
48. S. V. Krivovichev, C. L. Cahill and P. C. Burns, *Inorg. Chem.*, 2002, **41**, 34-39.
49. E. V. Alekseev, S. V. Krivovichev, T. Armbruster, W. Depmeier, E. V. Suleimanov, E. V. Chuprunov and A. V. Golubev, *Z. Anorg. Allg. Chem.*, 2007, **633**, 1979-1984.
50. S. V. Krivovichev and P. C. Burns, *Solid State Sci.*, 2003, **5**, 481-485.
51. S. V. Krivovichev, R. J. Finch and P. C. Burns, *The Canadian Mineralogist*, 2002, **40**, 193-200.
52. G. G. Sadikov, T. I. Krasovskaya, Y. A. Polyakov and V. P. Nikolaev, *Inorg. Mater.*, 1988, **24**, 91-96.
53. S. Krivovichev and P. Burns, *Can. Mineral.*, 2005, **43**, 713-720.
54. S. Obbade, S. Yagoubi, C. Dion, M. Saadi and F. Abraham, *J. Solid State Chem.*, 2003, **174**, 19-31.
55. E. Alekseev, E. Suleimanov, E. Chuprunov, A. Golubev, G. Fukin and M. Marychev, *Russian Journal of Inorganic Chemistry*, 2007, **52**, 1446-1449.
56. S. Yagoubi, S. Obbade, S. Saad and F. Abraham, *J. Solid State Chem.*, 2011, **184**, 971-981.
57. S. V. Krivovichev and P. C. Burns, *The Canadian Mineralogist*, 2003, **41**, 707-719.
58. V. N. Khrustalev, G. B. Andreev, M. Y. Antipin, A. M. Fedoseev, N. A. Budantseva and I. B. Shirokova, *Russian Journal of Inorganic Chemistry*, 2000, **45**, 1845-1847.
59. G. B. Andreev, M. Y. Antipin, A. M. Fedoseev and N. A. Budantseva, *Russian Journal of Coordination Chemistry*, 2001, **27**, 208-210.
60. S. Krivovichev and P. Burns, *Can. Mineral.*, 2001, **39**, 207-214.
61. J. V. Badding, *Annual Review of Materials Science*, 1998, **28**, 631-658.
62. H. D. Zhou, S. T. Bramwell, J. G. Cheng, C. R. Wiebe, G. Li, L. Balicas, J. A. Bloxsom, H. J. Silverstein, J. S. Zhou, J. B. Goodenough and J. S. Gardner, *Nat. Commun.*, 2011, **2**, 478.
63. F. Tassone, G. L. Chiarotti, R. Rousseau, S. Scandolo and E. Tosatti, *ChemPhysChem*, 2005, **6**, 1752-1756.

